

TESTING BLEND SCENARIOS FOR EXTRASOLAR TRANSITING PLANET CANDIDATES. II. — OGLE-TR-56

GUILLERMO TORRES¹, MACIEJ KONACKI², DIMITAR D. SASSELOV¹, SAURABH JHA³

Draft version September 23, 2018

ABSTRACT

We re-examine the photometric and spectroscopic evidence available for the star OGLE-TR-56, recently discovered to harbor a giant planet presenting transits and orbiting with a period of 1.21 days. We investigate the possibility that the observational signatures reported might be the result of “blending” with the light of an eclipsing binary along the same line of sight. Using techniques developed earlier we perform fits to the light curve under a variety of blend configurations, subject to all observational constraints, and we infer further properties of these possible blends. We then carry out realistic end-to-end simulations based on those properties in order to quantify the spectral line asymmetries and radial velocity variations expected from such scenarios. We confront these calculations with the observations. The results from these models are clearly inconsistent with the measured radial velocity and bisector span variations, ruling out blends and confirming the planetary nature of the companion. The example of OGLE-TR-56 serves to illustrate the sort of tests that can and should be performed on transiting planet candidates to eliminate the possibility of “false positives”, and in particular, line-of-sight contamination from eclipsing binaries.

Subject headings: binaries: eclipsing — line: profiles — planetary systems — stars: evolution — stars: individual (OGLE-TR-56) — techniques: radial velocities

1. INTRODUCTION

The search for extrasolar giant planets has entered an exciting new era, one in which these objects can be discovered indirectly by the tiny photometric signatures they produce as they transit across the disk of their parent star (periodic $\sim 1\%$ drops in brightness). Numerous photometric search programs are underway or under development worldwide (see Horne 2003). Six stars with transiting planets have been found so far: HD 209458 (Henry et al. 2000; Charbonneau et al. 2000), OGLE-TR-56 (Konacki et al. 2003a), OGLE-TR-113 (Bouchy et al. 2004; Konacki et al. 2004), OGLE-TR-132 (Bouchy et al. 2004), TrES-1 (Alonso et al. 2004), and OGLE-TR-111 (Pont et al. 2004).⁴ The OGLE-TR planets were originally detected as low-amplitude transit events by the most successful of the photometric surveys, OGLE-III (Optical Gravitational Lensing Experiment; Udalski et al. 2002b,c, 2003), and later confirmed by radial-velocity follow-up. The planet around HD 209458 was originally discovered by its radial velocity signature—the small reflex motion of the star in response to the pull from the planet—and only later was it found to undergo transits. It is the Doppler technique, in fact, that has been the most successful in discovering extrasolar planets, having produced more than 100 giant planets to date (Schneider 2004).

Both the Doppler and the transit search methods suf-

fer from the problem of astrophysical “false positives”, which refers to other phenomena that can produce the same observational signature but do not involve planets. In the case of the Doppler searches the concern is that similar velocity variations might result from chromospheric activity on the star (e.g., spots), sub-surface convection (granulation), other line asymmetries from undetected stellar companions, or even stellar oscillations (see, e.g., Gray 1997; Gray & Hatzes 1997; Gray 1998). For the transit searches the main contaminants are (1) eclipsing binaries with grazing geometry, (2) transits of a small star in front of a large star (such as an M dwarf passing in front of an F star, or a solar-type star in front of a giant), and (3) eclipsing binary systems with deep eclipses, blended with the light of another star along the same line of sight that dilutes the minima. In the latter case (referred to as a “blend”), the intruding star may or may not be physically associated with the binary. It is these blend scenarios that are the subject of this paper.

Cases that only involve an eclipsing binary with no contaminants (scenarios [1] and [2] above) are relatively easy to dismiss with radial velocity measurements since the expected amplitudes are typically several tens of km s^{-1} , as opposed to a few hundred m s^{-1} for the case of a Jupiter-mass planet around a solar-type star. Blend configurations, on the other hand, can be much more difficult to rule out as the main star may show little or no velocity variation at all, and may therefore appear to have a very low-mass companion in orbit when in reality it does not. This is particularly the case for very faint candidates ($V = 14\text{--}19$) such as those being reported from surveys such as OGLE-III (e.g., Udalski et al. 2002a), EXPLORE (Mallén-Ornelas et al. 2003), MACHO (Drake & Cook 2004), and others. For these objects the precision of the velocities is much lower than for the typically brighter stars ($V < 11$) that have been targeted in Doppler searches, and the potential for

¹ Harvard-Smithsonian Center for Astrophysics, 60 Garden St., Cambridge, MA 02138, USA

² California Institute of Technology, Div. of Geological & Planetary Sciences 150-21, Pasadena, CA 91125, USA

³ Department of Astronomy, University of California, Berkeley, CA 94720, USA

Electronic address: gtorres@cfa.harvard.edu

⁴ Another case, OGLE-TR-3, was reported recently by Dreizler et al. (2003) and claimed to harbor a transiting planet with a period of 1.19 days, but additional studies showed that it is most likely a false positive (Konacki et al. 2003b).

confusion is greater because they also tend to be in very crowded fields. It is therefore important to examine these cases very carefully.

In a recent paper (Torres et al. 2004b, hereafter Paper I) we described a procedure to model the light curves of transit candidates as the combination of three stars forming the blend, and we applied it to the case of OGLE-TR-33, a candidate that turned out to be a false positive. We showed how such modeling tools allow one to predict other observable properties of the blend and can become a useful guide to look for additional signs of a contaminating eclipsing binary. One such sign that can easily be overlooked is asymmetries in the spectral lines, which can lead to spurious velocity measurements. In the present paper we develop procedures to simulate line asymmetries and their effects on the measured velocities of a transit candidate resulting from typical blend scenarios. We illustrate these techniques by carrying out a critical examination of the case of OGLE-TR-56 ($V = 16.6$), the first extrasolar transiting planet to emerge from the lists of very faint candidates, and the one with the shortest orbital period so far (1.21 days). We perform blend simulations subject to all observational constraints in an attempt to explain the system as a false positive, but despite all our efforts we are unable to find a plausible configuration involving a contaminating eclipsing binary that does not violate one or another of those constraints by a large margin. This lends further support to the planetary nature of the companion of OGLE-TR-56.

2. OGLE-TR-56: THE SPECTROSCOPIC EVIDENCE

The original detection of periodic transit-like events in OGLE-TR-56 was reported by Udalski et al. (2002b). The star was part of the second batch of candidates produced by the OGLE-III photometric survey, which targeted three fields toward the Galactic center. High-resolution spectroscopic follow-up observations were conducted by our team in July 2002, and small but significant radial velocity variations were announced by Konacki et al. (2003a) on the basis of measurements on three nights near the quadratures, implying the presence of a planetary-mass object in orbit. As the first such claim among all the transit candidates reported until then—and by far the faintest candidate ever considered to have a chance of harboring a planet—those results were carefully scrutinized by the community and were received quite understandably with a measure of skepticism. The initial concerns on the observational side regarding this particular detection focussed on two issues: (a) The *reality* (or statistical significance) of the radial velocity variations, especially since the claim was based on only 3 averaged measurements; and (b) the *interpretation* of the velocity variations, given the crowding in the field and the increased probability of a blend.⁵

Such concerns are likely to be repeated for other faint

⁵ Two additional concerns have to do with (c) whether a planet in such a tight orbit such as OGLE-TR-56 can exist at all (which theory appears not to rule out; see Trilling et al. 1998; Baraffe et al. 2004), and (d) why Doppler searches among brighter stars have not found additional examples in very short-period orbits (≤ 2.5 days) despite being sensitive to them. The latter may perhaps be the result of a much lower frequency of occurrence of these “very hot Jupiters”, coupled with very strong selection toward short periods in transit surveys such as OGLE (see Bouchy et al. 2004; Gaudi, Seager, & Mallén-Ornelas 2004).

candidates that might be confirmed in the future, and it is therefore necessary to consider them very seriously. The first concern is related mostly to errors of measurement (accidental or systematic), and whether the results might be due, for example, to limitations in the reduction and/or analysis techniques or to the stability of the spectrograph employed (in this case, HIRES on the Keck I telescope; Vogt et al. 1994). For OGLE-TR-56 these issues were addressed by Konacki et al. (2003b), who showed that systematic errors in the velocities are no more than about 100 m s^{-1} and accidental errors are somewhat smaller, making the reported peak-to-peak velocity change (initially estimated to be $\sim 340 \text{ m s}^{-1}$) statistically significant considering that the phasing in the orbit is known and fixed from the photometry. Eight additional measurements with the same instrument were reported more recently by Torres et al. (2004a), and show even more clearly that the velocity is changing as expected from the phasing in the orbit. The revised amplitude folding together all the measurements is larger than originally estimated, but it is now much better characterized (peak-to-peak variation near 600 m s^{-1}). More importantly, independent confirmation of velocity variations has been reported by another group using different instrumentation. Mayor et al. (2003) obtained five measurements of OGLE-TR-56 during the commissioning of the new HARPS instrument on the ESO 3.6-m telescope in June of 2003, achieving a nominal precision of about 30 m s^{-1} . Their preliminary analysis gives much the same amplitude as Torres et al. (2004a).

With the reality of the velocity variations now beyond doubt, the issue of their interpretation becomes the main concern for OGLE-TR-56, and is the motivation for the remainder of this paper. Can the observations be explained by a blend scenario, with an eclipsing binary along the same line of sight contaminating the light of the main star? If so, the velocity variations measured would be caused by blending with the spectral lines from the primary of the eclipsing binary moving back and forth relative to the main star, with a period of 1.21 days. Are these extra lines visible in the spectra? Strong and variable line asymmetries are also to be expected from such a scenario. Are the measured asymmetries (Torres et al. 2004a) consistent with a blend model? Given the importance of OGLE-TR-56 as the first example of a seemingly new class of planetary objects under extreme conditions of proximity to the parent star, the answers to the questions above must be *quantitative* rather than *qualitative*. We begin in the next section by modeling the light curve in detail following the procedures we introduced in Paper I for OGLE-TR-33.

3. LIGHT CURVE FITS TO OGLE-TR-56 UNDER A BLEND SCENARIO

The shape of a light curve showing transit-like events contains valuable information that can be used in some cases to recognize false positive scenarios. For example, Drake (2003) and Sirko & Paczyński (2003) showed that the variations outside of eclipse, as measured from a Fourier analysis, can often indicate that the companion is stellar as opposed to substellar, from effects due to tidal distortions, reflection, or gravity brightening. An isolated eclipsing binary (e.g., one with grazing geometry, or consisting of a small star passing in front of a

much larger star) can be ruled out as the explanation for the light curve of OGLE-TR-56 because of the very small velocity amplitude measured. However, an eclipsing binary blended with another star remains a possibility, in principle, and some of its properties could still show through in the light curve, even though they would be diluted. But as reported by the authors above, the Fourier decomposition test for OGLE-TR-56 comes out negative, indicating no significant curvature outside of eclipse.

A different kind of test was proposed by Seager & Mallén-Ornelas (2003) based on the morphology of the transits themselves. They showed that the mean density of the primary star, as well as the radius of the companion, can be estimated by careful measurement of the depth of the transit (relative change in flux, ΔF), its total duration (t_T), and the duration of the flat portion (t_F), along with the knowledge of the orbital period. Any inconsistency in the mean density with values for normal (main-sequence) stars, or with additional information available for the primary, would be an indication of a blend. Once again this test comes out negative for OGLE-TR-56. We measure $\Delta F = 0.016$, $t_T = 0.060$, and $t_F = 0.036$ (the latter two in phase units), which when combined with the orbital period of 1.2119189 days (Torres et al. 2004a) lead to a primary star very similar to the Sun in mean density, as well as in both mass and radius when a typical mass-radius relation for main sequence stars is adopted. Indeed the temperature estimated for OGLE-TR-56 from our high-resolution spectra is solar-like (~ 5900 K; Sasselov 2003).

More detailed information on the properties of a possible blend can be obtained from a direct fit to the light curve as described in Paper I. Briefly, the photometry is modeled using the eclipsing binary computer code EBOP (see Nelson & Davis 1972; Etzel 1981; Popper & Etzel 1981), fully accounting for effects such as stellar oblateness, reflection, limb darkening, and gravity brightening. The properties of the three stars composing the blend (which are assumed to be on the main sequence) are parameterized in terms of their mass and are constrained to fit suitable model isochrones. These isochrones may be different for the binary and for the main star if they do not form a physical triple system. In that case, differential extinction must also be accounted for since they can be at different distances from the observer. All other relevant properties of the stars such as their radii and luminosities are taken also from the isochrones (see Paper I for details). The important advantage of this procedure is that it allows testable predictions for some of the other properties of the eclipsing binary that are potentially observable. These properties include the brightness of the primary in the eclipsing binary relative to the main star, its velocity semi-amplitude, and its projected rotational velocity (assuming its spin is synchronized with the orbital motion). This was illustrated in Paper I with the example of the blend case OGLE-TR-33. The same procedure is applied here to OGLE-TR-56.

As in Paper I we make use of the model isochrones by Girardi et al. (2000) to describe the properties of the stars in the blend⁶. The photometric data for OGLE-TR-

56 are described by Torres et al. (2004a), and we adopt the measurement errors reported by the OGLE team⁷. Those observations were made in the I band. We begin by assuming the eclipsing binary and the third star are physically associated, and we therefore use the same isochrone for both with an adopted age of 3 Gyr (Sasselov 2003) and solar metallicity ($Z = 0.019$). We refer to this model as **MODEL1**. We follow the notation of Paper I and refer to the primary and secondary in the eclipsing binary as star 1 and star 2, respectively, while the main star that dilutes the eclipses of the binary is referred to as star 3. We assign to star 3 a mass on the isochrone such that the corresponding temperature agrees with the spectroscopic determination for OGLE-TR-56 ($M_3 = 1.05 M_\odot$, $T_{\text{eff}} = 5900$ K). The inclination angle is assumed to be 90° for simplicity.

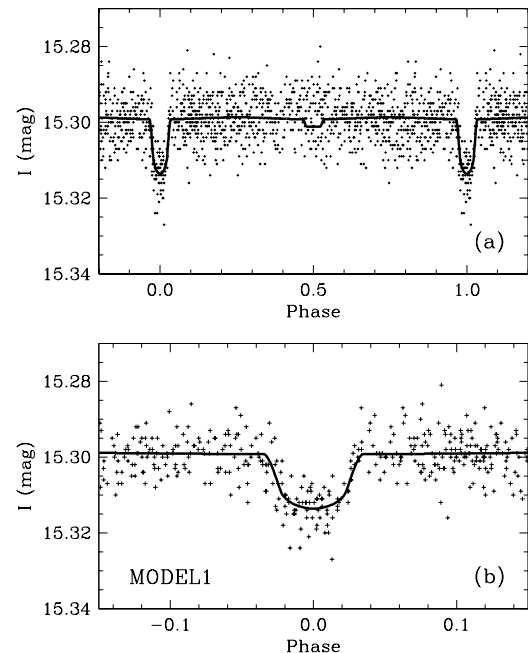


FIG. 1.— (a) Blend model fit to the light curve of OGLE-TR-56 (**MODEL1**). The main star (star 3) and the contaminating eclipsing binary are assumed to be physically associated (age = 3 Gyr). The masses of the stars in the eclipsing binary (star 1 and star 2) are $M_1 = 0.89 M_\odot$ and $M_2 = 0.13 M_\odot$, and star 3 contributes 71% of the light in the I band. The predicted light ratio in the visual band is $L_1/L_3 = 0.35$. (b) Enlargement of the primary eclipse.

tion, in the opacities, in the equation of state, and the use of gray boundary conditions, all of which become very important in the lower main sequence. In particular, theoretical radii from these and all current stellar evolution models are known to be underestimated by 10% or more compared to measurements of well-studied low-mass eclipsing binaries (see, e.g., Torres & Ribas 2002; Ribas 2003). While other models for cool stars are somewhat more sophisticated (e.g., Siess, Forestini & Dougados 1997; Baraffe et al. 1998), our reason for choosing this particular set of isochrones is that they span the largest range of masses for our application, beginning at $0.15 M_\odot$. Despite this, slight extrapolations to even lower masses were necessary in some cases. Given the importance of the model radii in our simulations for determining key properties of the eclipses such as their depth and duration, we have attempted to bring them into closer agreement with the radii of real stars by applying ad-hoc corrections based on a careful comparison with accurately measured radii for late-type stars. The correction factors are mass-dependent, and average 1.1 over the mass range of interest for our work.

⁶ For low-mass stars these models become increasingly unrealistic partly because of shortcomings in the treatment of convec-

⁷ See <http://bulge.princeton.edu/~ogle/ogle3/transits/ogle56.html>, and Kruszewski & Semeniuk (2003).

Our blend model adjusted to the light curve is shown in Figure 1. The resulting properties of the stars in the eclipsing binary are $M_1 = 0.89 M_{\odot}$ (approximately spectral type G8 V) and $M_2 = 0.13 M_{\odot}$ (M4-5 V), and the inferred distance to the system is ~ 1.8 kpc. Very shallow secondary eclipses only 0.002 mag deep are also predicted by this model, but they are undetectable given the precision of the observations (typical errors of ~ 0.006 mag for an individual measurement). We note that the fit to the primary eclipse with this blend model is essentially indistinguishable from a fit that models a true planetary transit (see Torres et al. 2004a, Figure 4). Thus, the shape of the light curve alone is insufficient to discriminate between the two. The fitting procedure provides all the physical properties of star 1 from the isochrone, so that it is possible to estimate the semi-amplitude of its radial-velocity orbit ($K_1 = 26 \text{ km s}^{-1}$) and also its projected rotational velocity ($v_1 \sin i = 36 \text{ km s}^{-1}$), under the plausible assumption that it is synchronized with the orbital motion (given the short orbital period). The brightness of star 1 relative to the main star is predicted to be $L_1/L_3 = 0.35$ in the visual band⁸. The latter quantity conflicts with the spectroscopic observations for OGLE-TR-56, which place an upper limit on the presence of lines from another star in the spectrum of about 3% of the light of the main star (Konacki et al. 2003b). A star as bright as 35% of the light of star 3 would be fairly obvious in the spectra, despite the rotational broadening. We conclude that this particular blend scenario is inconsistent with the data⁹. Additional difficulties with MODEL1 arise from the magnitude of the line asymmetries that are expected. We defer the discussion of these issues to §4.

Since the main problem with MODEL1 seems to be the excessive brightness of star 1, we explored ways of making star 1 fainter while still providing a reasonably good fit to the light curve. One such way is to remove the requirement that the eclipsing binary and the main star be in a physical triple, and to allow the binary to be in the background. In this case the age of the isochrone for the binary can in principle be different. For lack of a better estimate we retain the 3 Gyr isochrone for both, but the binary is no longer constrained to be at the same distance as star 3. We performed extensive modeling of the photometry for a range of distances between the binary and star 3 parameterized, for convenience, in terms of the difference in distance modulus ΔM (see Paper I). We assumed an edge-on orientation, as before. The results are summarized in Figure 2, where we show how the parameters of star 1 and star 2 change as the binary is placed farther behind star 3. As expected the observed light ratio L_1/L_3 decreases with distance (Figure 2b), and reaches the upper limit determined spectroscopically

⁸ The symbol L is used throughout this paper to denote brightness (“light”).

⁹ Tests show that adjusting the age of the isochrone does not qualitatively change the conclusion. With increasing age L_1/L_3 decreases somewhat as star 3 evolves upward in luminosity, but not enough before a star with a mass appropriate for the temperature of OGLE-TR-56 leaves the main sequence altogether. The latter occurs for ages greater than about 7 Gyr, at which L_1/L_3 has only decreased to approximately 0.20. Further tests with lower inclination angles for the binary show that the L_1/L_3 increases as the system departs from an edge-on orientation, making the disagreement with the observations even worse.

(0.03) at $\Delta M \approx 2.0$ (binary approximately 2.3 kpc behind star 3; Figure 2a). We refer to this solution as MODEL2, and indicate it with squares in the figure. The mass of star 1 that provides the best fit has increased at this distance by about 12% compared to MODEL1, while that of star 2 is more than a factor of 3 larger than before (Figure 2d). The reason for these changes can be understood as follows. As the binary is pushed back and its contribution to the total light decreases, the eclipse becomes more diluted (shallower), and so in order to maintain the observed depth the relative size of the secondary in the binary (star 2) must increase relative to the primary (star 1), which implies increasing the mass of star 2. This, in turn, will affect the total duration of the eclipse for a fixed star 1, both from the change in the relative size of star 2 and star 1, and from the change in semimajor axis for a fixed orbital period (see Seager & Mallén-Ornelas 2003). In order to conform to the observed transit duration, the mass and size of star 1 then need to increase slightly to compensate. Accordingly, the predicted $v \sin i$ of star 1 shows only a small dependence with ΔM , while K_1 varies significantly as the mass of the companion increases. The quality of the fits degrades as the binary is placed farther in the background (Figure 2f), but remains more or less acceptable at $\Delta M = 2.0$. That fit is shown later in Figure 4a along

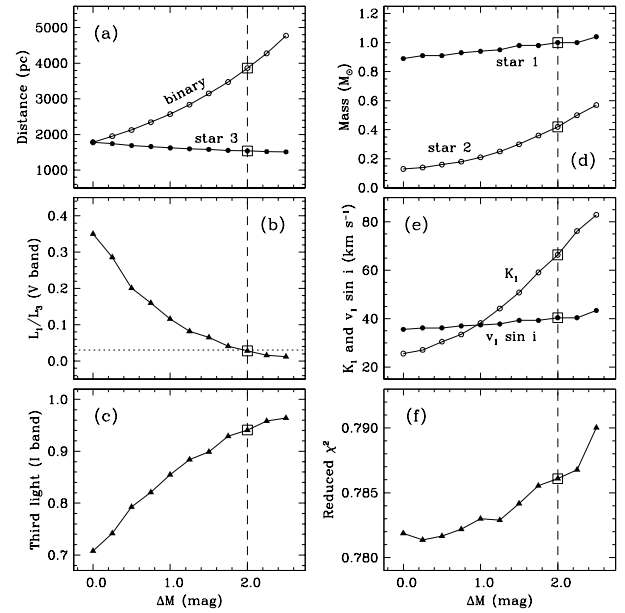


FIG. 2.— Results from a grid of light curve fits to the photometry of OGLE-TR-56, with the eclipsing binary placed at increasing distances behind the main star (star 3), as parameterized by the difference in the distance modulus ΔM . The fit marked with squares is referred to in the text and in Table 1 as MODEL2. The leftmost points correspond to MODEL1. (a) Fitted distance in parsecs to the binary and to star 3; (b) Light ratio L_1/L_3 in the visual band. The horizontal dotted line represents the upper limit estimated from the high-resolution spectra ($\sim 3\%$); (c) Contribution of star 3 to the total light in the I band (“third light” in eclipsing binary terminology); (d) Best fit masses for the primary and secondary in the eclipsing binary; (e) Predicted radial velocity semi-amplitude and projected rotational velocity for the primary in the eclipsing binary (star 1); (f) Reduced χ^2 for the solution (that the values are lower than unity suggests the photometric errors are slightly overestimated).

with the light curve from MODEL1 for comparison. The consequences of MODEL2 for the line asymmetries and expected velocity variations are explored in the next section.

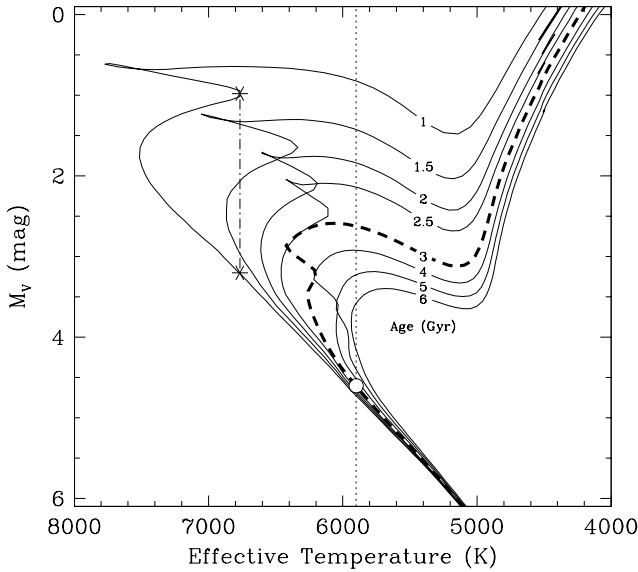


FIG. 3.— Isochrones from the Yonsei-Yale series of evolutionary models (Yi, Kim, & Demarque 2003) for a range of ages labeled in Gyr. The 3 Gyr isochrone for OGLE-TR-56 is represented with a heavy dashed line. As an example, the asterisks show two possible locations of a main-sequence star at a fixed age with the same effective temperature, but with brightness differing by about 2 mag. The effect of choosing the brighter location for star 3 in a blend model would be to decrease L_1/L_3 . The open circle on the 3-Gyr isochrone corresponds to the position of OGLE-TR-56 on the main sequence, at the measured temperature of 5900 K (vertical dotted line). At these low temperatures the flexibility of choosing the brighter of two vertically aligned locations for star 3 with significantly different brightness is effectively eliminated because of the change in the shape of the isochrones.

If we wish to keep the three stars at the same distance, as in a triple system, an alternate way of decreasing the relative brightness of star 1 to comply with the spectroscopic constraint is to make star 3 itself intrinsically *brighter*, e.g., by evolving it from the zero-age main sequence. There are good reasons for assuming physical association that have to do with the apparent symmetry of the velocity variations (see §4). The brightness change required here is roughly a factor of 10 (about 2.5 magnitudes) in order to reduce the brightness ratio L_1/L_3 from 0.35 (MODEL1) to the observational upper limit of 0.03 (Konacki et al. 2003b). A similar situation was described in Paper I for the case of OGLE-TR-33, where it was shown that by fine-tuning the age an isochrone could be found in which a slightly more evolved star 3 could be about 2 magnitudes brighter at the same effective temperature (constrained by the spectroscopy). The location of star 3 in the H-R diagram would be beyond the turnoff but still on the main sequence, near the point of hydrogen exhaustion (see Figure 5 of Torres et al. 2004b). OGLE-TR-56 is cooler than OGLE-TR-33, however, and a glance at the morphology of the isochrones reveals that a similar argument does not work for a temperature of

5900 K, at any age. This is illustrated in Figure 3, where instead of the Girardi et al. (2000) models we have used those of Yi, Kim, & Demarque (2003) for their finer resolution near the turnoff. It is seen, for example, that the “blue hook” feature gradually disappears for older ages, reducing the difference in brightness between its red end (coolest and most luminous point on the main sequence beyond the turnoff) and a location below it with the same temperature. The change in shape as the age increases coincides with the disappearance of convective cores at masses slightly larger than the Sun. Unless one is willing to accept that OGLE-TR-56 is in the rapid phase of evolution often referred to as the Hertzsprung gap (horizontal portions of the isochrones where stars are evolving mostly toward cooler temperatures without changing their brightness significantly), the brightness of star 3 cannot be much larger than indicated by the open circle, at its location on the main sequence.

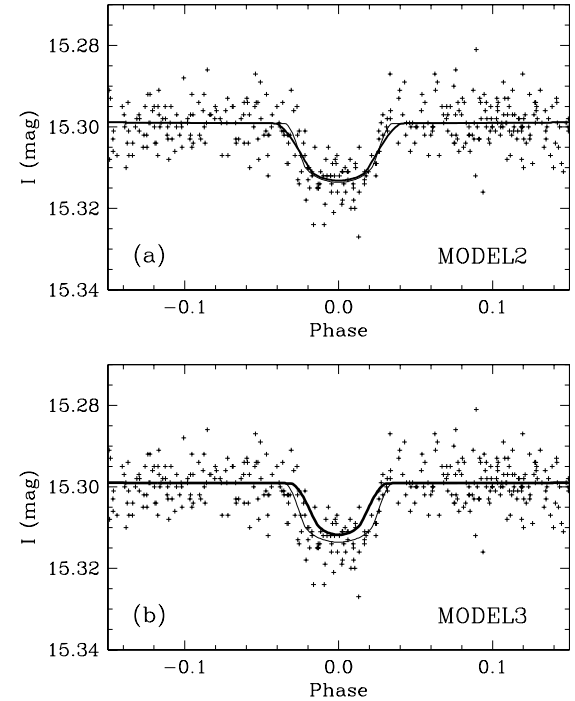


FIG. 4.— Two blend models for OGLE-TR-56 (thick lines) that satisfy the spectroscopic constraint on the brightness of star 1 relative to star 3 in the V band ($\leq 3\%$). The fit for MODEL1 from Figure 1b is superimposed in each panel for reference (thin line). (a) MODEL2, in which the binary is in the background of star 3 (~ 2.3 kpc behind, in this case; see Figure 2). (b) MODEL3, in which the binary and star 3 are at the same distance (as in a physical triple), but star 1 is constrained to have a brightness of 3% relative to the main star.

For completeness we explored also a blend scenario in which the three stars form a physical triple system, but star 1 is constrained to have a relative brightness in the V band consistent with the upper limit from spectroscopy ($\sim 3\%$). Only the properties of star 2 were adjusted, and we refer to this as MODEL3. The inclination angle was again fixed at 90° , and the adopted age is the same as before (3 Gyr), although this does not qualitatively change the results. This solution is noticeably worse than the previous two (reduced χ^2 about 8% larger), but at least it still reproduces the total duration and depth of the

TABLE 1

Parameter	MODEL1	MODEL2	MODEL3
$M_1 (M_\odot)$	0.89	1.00	0.60
$M_2 (M_\odot)$	0.13	0.42	0.22
$L_1/L_3 (V \text{ band})$	0.35	0.03	0.03
$L_3/L_{\text{tot}} (I \text{ band}) (\%)^a$	71	94	94
$K_1 (\text{km s}^{-1})$	26	66	50
$v_1 \sin i (\text{km s}^{-1})$	36	40	26
Distance to star 3 (kpc)...	1.78	1.54	1.54
Distance to binary (kpc)...	1.78	3.86	1.54
ΔM (mag) ^b	0.00	2.00	0.00
a_v (mag kpc^{-1}) ^c	0.56	0.66	0.66
Reduced χ^2 of the fit ^d	0.78188	0.78609	0.84734

^aRelative contribution of star 3 to the total light of the system.

^bDifference in the distance modulus between the binary and star 3.

^cCoefficient of differential extinction in the V band, adjusted to reproduce the observed system magnitudes in the V and I bands (see Paper I).

^dThe values significantly lower than unity imply that the measurement errors are slightly overestimated, by roughly 10%.

eclipse tolerably well (see Figure 4b). We summarize the properties of this and the other two models in Table 1.

As in the case of the first scenario, MODEL2 and MODEL3 predict shallow secondary eclipses with depths of ~ 0.002 mag and ~ 0.006 mag, respectively, which would be difficult to see.

4. SIMULATING LINE ASYMMETRIES AND RADIAL VELOCITY VARIATIONS

In blend scenarios such as those modeled in the previous section the presence of lines from another star in the spectrum of OGLE-TR-56 will affect the measurement of the radial velocities to some degree. As mentioned above this is due to asymmetries introduced in the profiles of the main star. The extent to which these asymmetries will distort the radial velocities depends on the brightness of the secondary lines and their relative displacement. Intrinsic broadening may also be a factor. Quantitative measures of the asymmetries for planet candidates showing velocity variations are now often reported in the literature, and in many cases they have turned out to be small. We believe, however, that this alone is not sufficient evidence against a blend. In this section we explore the magnitude of these effects by means of simulations to see whether they can explain the measurements reported for OGLE-TR-56 by Torres et al. (2004a).

A similar philosophy was adopted by Santos et al. (2002) to investigate small radial velocity variations and line asymmetries found in the case of the star HD 41004. This is a close visual binary initially thought to have a planetary companion around the primary star based on high-precision Doppler monitoring performed by those authors. The visual binary with an angular separation of $0.^{\circ}5$ was unresolved at the spectrograph, effectively making it a blend. Unlike the case of OGLE-TR-56, however, there is no transit signature in HD 41004 and therefore there is less information about the stars and the geometry of the system. Santos et al. (2002) approximated the cross-correlation functions of the two stars in HD 41004 with Gaussians, and sought to reproduce the measured velocity and bisector variations by combining two Gaus-

sians with appropriate parameters to simulate the measured correlation functions. From numerical experiments they were able to infer the key parameters of the system, and to fully explain the observations as the result of a possible brown dwarf orbiting the visual companion instead of a planet around the primary star. Their results for the physical and orbital properties of the visual companion were subsequently corroborated by Zucker et al. (2003).

In this paper the situation is somewhat different in that our blend models fitted to the light curve of OGLE-TR-56 constrain many of the key properties of the stars. Our goal is then to see if these inferred properties lead to a consistent picture of velocity and asymmetry variations matching what is observed. In addition, we wish to be as realistic as possible in approximating the observations. Therefore, instead of adopting Gaussian profiles for the correlation functions, we simulate composite spectra guided by the models in §3, by combining together calculated spectra for star 1 and star 3 that conform to the stellar and orbital characteristics implied by each blend scenario. We then measure radial velocities by cross-correlation and estimate spectral line asymmetries in these artificial spectra in exactly the same way as was done for the original observations of OGLE-TR-56.

For star 3 the calculated spectrum we used is the same one adopted by Torres et al. (2004a), which was derived from a fit to the observed spectrum of OGLE-TR-56, and was used in that work as the template for the cross-correlations. This calculated spectrum has an effective temperature of 6000 K, surface gravity $\log g = 4.5$, and projected rotational velocity $v \sin i = 3 \text{ km s}^{-1}$. For a given blend model star 1 is assigned the temperature and surface gravity inferred from the isochrone for its mass, and a rotational velocity given by the predicted value of $v_1 \sin i$. Star 1 was then scaled down by the predicted light ratio L_1/L_3 , and Doppler-shifted before adding it to the spectrum of the main star. The shift between star 1 and star 3 is controlled by the velocity amplitude of star 1 in its orbit (K_1) and the difference $\Delta\gamma$ between its center-of-mass velocity and the (presumably constant) velocity of star 3. Since the period and epoch of transit are well known, the Doppler shift can be computed for any instant of time. $\Delta\gamma$ is a free parameter in principle, although for scenarios such as MODEL1 and MODEL3 it is expected to be small compared to K_1 given that the configuration is assumed to be a hierarchical triple system.

In an effort to approximate the real observations of OGLE-TR-56 as closely as possible, the artificial composite spectra were divided into sections corresponding precisely to each of the echelle orders of the original observations (see Konacki et al. 2003b), and rebinned to exactly the same number of pixels as in the real data prior to further analysis. The calculated spectra were initially generated at much higher spectral resolution than the real observations (by a factor of ~ 10), and then broadened with the average instrumental profile of the Keck spectrograph, which was assumed to be Gaussian in shape and with $\text{FWHM} = 4.6 \text{ km s}^{-1}$.

Radial velocities from these artificial composite spectra were measured by cross-correlation using the IRAF¹⁰

¹⁰ IRAF is distributed by the National Optical Astronomy Observatories, which is operated by the Association of Universities

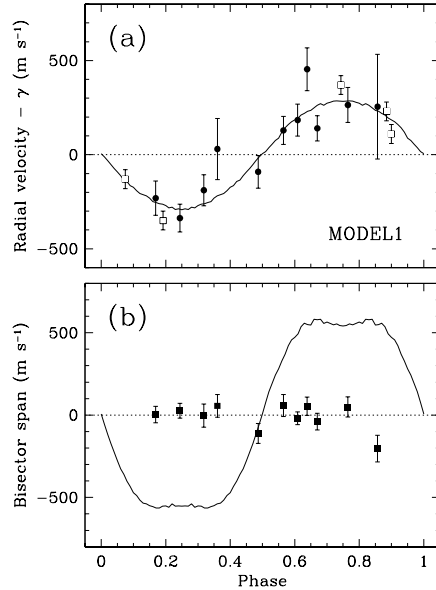


FIG. 5.— Simulated velocity and bisector span variations (solid curves) from the blend scenario described by MODEL1, compared with the measurements of OGLE-TR-56 from Torres et al. (2004a). (a) Radial velocity variations, with the center-of-mass velocity γ subtracted. The preliminary velocities from Mayor et al. (2003) are shown also for completeness (open squares). (b) Bisector span variations.

task XCSAO (Kurtz & Mink 1998), combining the results for all orders. The template used is the same as for the real observations (Torres et al. 2004a), and it happens to be the same spectrum used to model star 3. Line asymmetries were quantified by computing the line bisectors (e.g., Gray 1992) directly from the co-added correlation function, which is representative of the average spectral line. We then calculated the velocity difference in the bisector at two different correlation levels, which we refer to as the “bisector span”.¹¹ This is analogous to the definition employed by Queloz et al. (2001) and Santos et al. (2002).

We first simulated MODEL1, sampling all phases of the binary orbit and assuming $\Delta\gamma = 0 \text{ km s}^{-1}$. The results are shown in Figure 5, and are compared with the radial velocity observations and bisector spans reported for OGLE-TR-56 by Torres et al. (2004a). The top panel indicates an excellent agreement with the measured velocities, which is however only a coincidence. The lower panel shows that the asymmetries expected from this scenario are much larger than observed. The predicted bisector spans can reach velocities exceeding $\pm 500 \text{ m s}^{-1}$ near the quadratures, while the observations show no significant variation at all within the errors. Thus MODEL1 fails to reproduce the observations, as was already an-

for Research in Astronomy, Inc., under contract with the National Science Foundation.

¹¹ The particular correlation levels used here, 0.2 and 0.4, were chosen from the properties of the correlation functions for the observations of OGLE-TR-56. Levels below 0.2 are affected by noise, and levels above 0.4 are not measurable for some of the weaker exposures in which the peak of the correlation function does not reach that value. Our conclusions below are qualitatively unaffected by choosing different levels between these two values, so long as the simulations use the same levels.

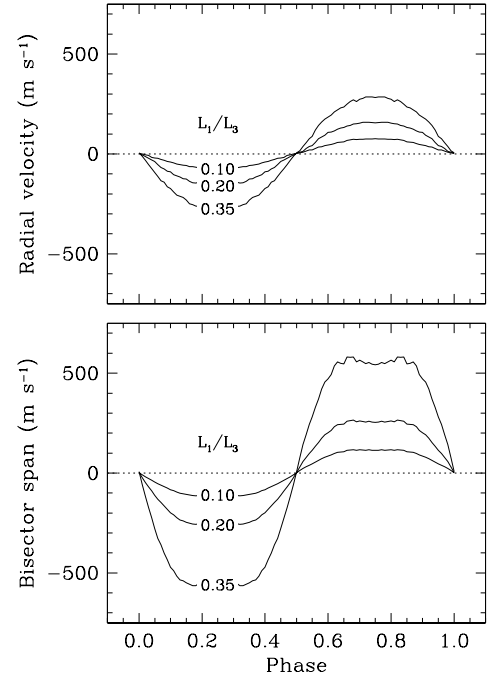


FIG. 6.— Effect of the light ratio L_1/L_3 (in the V band) upon the expected radial velocity variations and bisector spans from a blend scenario. $L_1/L_3 = 0.35$ corresponds to MODEL1, and the remaining parameters of the simulations are held at their values in that model (see Table 1).

ticipated in §3 from the excessive brightness of star 1 relative to star 3 ($L_1/L_3 = 0.35$).

Next we explored the sensitivity of the radial velocity and bisector span variations to the main parameters of the blend, in an attempt to understand their effect. We carried out extensive simulations over a broad range of values of L_1/L_3 , K_1 , $\Delta\gamma$, and $v_1 \sin i$, varying one parameter at a time and leaving the others fixed at their nominal values for MODEL1. A sampling of these tests is described below.

The effect of imposing different ratios L_1/L_3 for the brightness of the primary of the eclipsing binary relative to the main star in the visual band is shown in Figure 6. As expected the amplitude of the variations scales with the brightness of star 1, although not quite linearly.

Changing the semi-amplitude K_1 results in relatively minor changes in the amplitudes, but significant changes in the shape of the simulated curves both for the bisector span and the velocities, as seen in Figure 7. For small values of K_1 the lines of star 1 remain within the wings of those of the main star at all phases, and the curves are nearly sinusoidal. As K_1 increases, the lines of star 1 shift out of the wings of star 3 at the quadratures, and the effect is smaller at those phases producing a flattening out of the curves. They become increasingly non-sinusoidal with larger values of K_1 . Santos et al. (2002) described the same effect in their simulations.

Both the amplitude and the shape of the predicted velocity variations and bisector span variations depend very sensitively on the rotational broadening of star 1. This is illustrated in Figure 8. Sharper lines for star 1

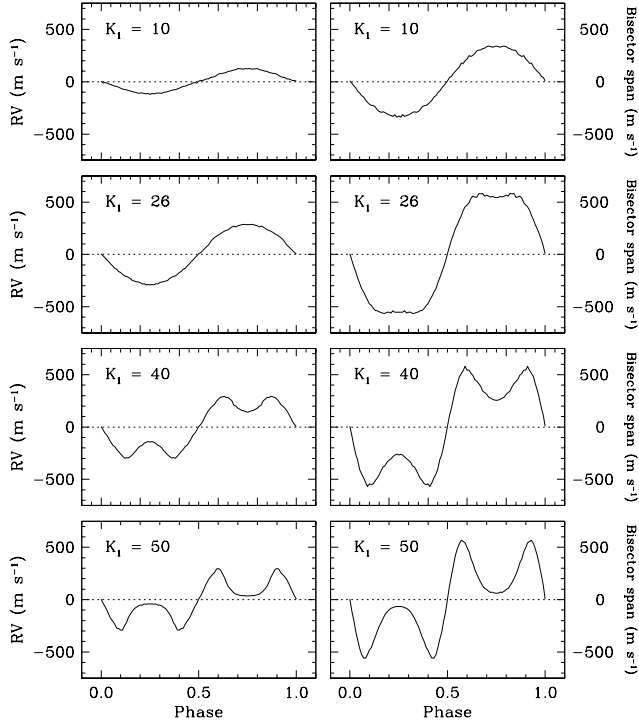


FIG. 7.— Effect of varying the semi-amplitude K_1 (in km s^{-1}) upon the expected radial velocity variations (left panels) and bisector spans (right panels) from a blend scenario. $K_1 = 26 \text{ km s}^{-1}$ corresponds to MODEL1, and the remaining parameters of the simulations are held at their values in that model (see Table 1).

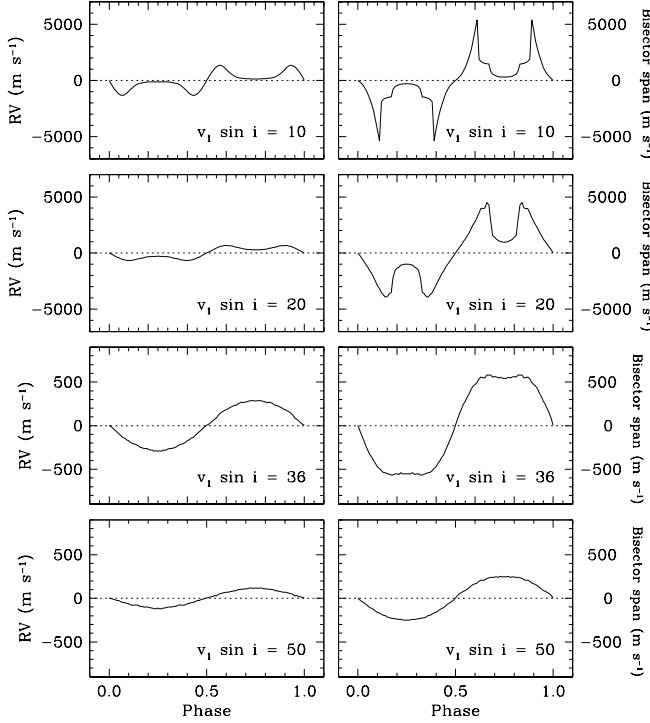


FIG. 8.— Effect of $v_1 \sin i$ (in km s^{-1}) on the expected radial velocity variations (left panels) and bisector spans (right panels) from a blend scenario. Note the change in the vertical scale for the bottom two panels on each side (see text). MODEL1 has $v_1 \sin i = 36 \text{ km s}^{-1}$. The remaining parameters of the simulations are held at their values in that model (see Table 1).

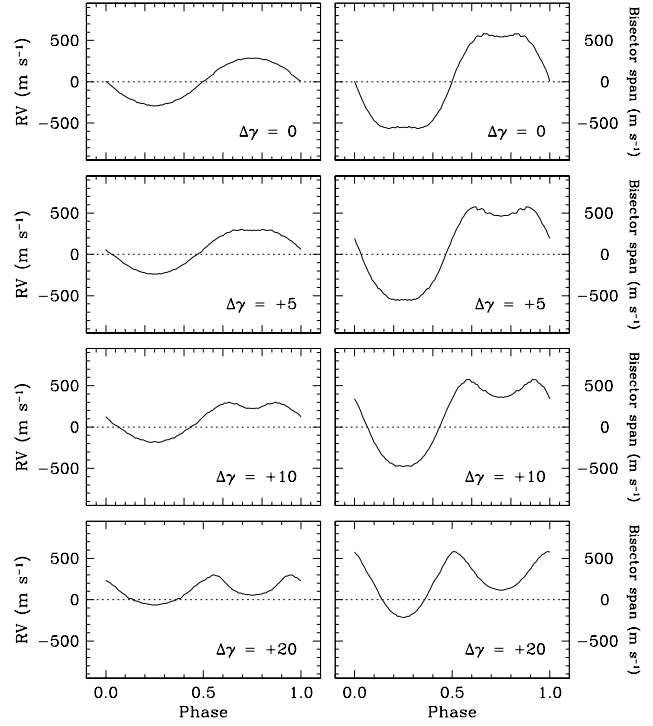


FIG. 9.— Effect of $\Delta\gamma$ (in km s^{-1}) on the expected radial velocity variations (left panels) and bisector spans (right panels) from a blend scenario. MODEL1 has $\Delta\gamma = 0 \text{ km s}^{-1}$. The remaining parameters of the simulations are held at their values in that model (see Table 1).

give larger variations except near the quadratures (for $K_1 = 26 \text{ km s}^{-1}$, as in MODEL1), as might also be expected. This leads to cusps in the curves that are progressively closer to phase 0.0 and 0.5 as the rotational velocity becomes smaller, qualitatively resembling the effect of a larger K_1 value. As $v_1 \sin i$ increases, the effect is attenuated due to the broader lines and the curves approach a more sinusoidal shape. In particular, a large drop in amplitude is observed between $v_1 \sin i$ of 20 km s^{-1} and 30 km s^{-1} , coincident with the point at which the rotation numerically exceeds the value of K_1 .

Finally, a change in $\Delta\gamma$ produces another qualitative distinction, this time an asymmetric shape to the bisector span and velocity variations that depends upon the sign of $\Delta\gamma$. This is shown in Figure 9. As a result, blend models that do not assume physical association between the eclipsing binary and the main star (such as MODEL2) would be expected to show asymmetrical shapes to the bisector and velocity variations, since $\Delta\gamma$ can be arbitrarily large in those cases. The measured velocity variations for OGLE-TR-56 appear to be more or less sinusoidal (c.f. Figure 5), and therefore values of $\Delta\gamma$ significantly different from zero (of order 10 km s^{-1} or greater, given the number of observations and their uncertainties) would seem to be inconsistent with the observations. Similarly, values of K_1 much larger than that used in MODEL1 would lead to a shape to the radial velocity curve in disagreement with the observations.

In Figure 10 we show the simulated bisector span and velocity variations resulting from the blend scenarios described by MODEL2 and MODEL3, along with the obser-

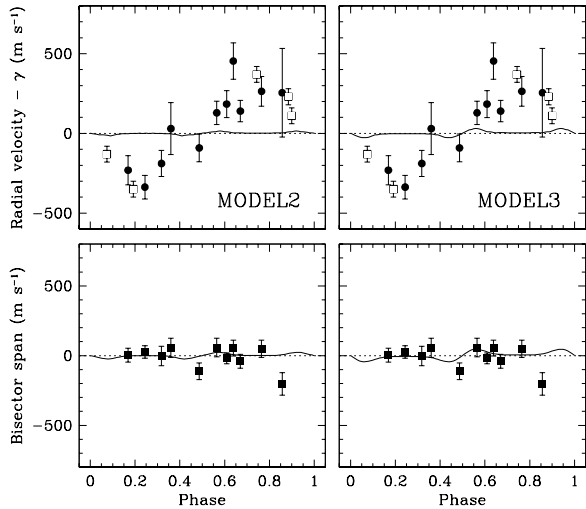


FIG. 10.— Simulated radial velocity and bisector span variations (solid curves) from the blend scenarios described by MODEL2 and MODEL3, compared with the measurements of OGLE-TR-56 from Torres et al. (2004a) and Mayor et al. (2003). Details and symbols are as in Figure 5.

vations. The expected bisector variations from MODEL2 are less than about 25 m s^{-1} . This is actually consistent with the observations, which show no appreciable change in the symmetry of the lines within the errors. However, the predicted velocity variations from this blend scenario are *also* very small, with a semi-amplitude less than 15 m s^{-1} , which is about 20 times smaller than observed. MODEL3 does not fare much better, with a bisector semi-amplitude under 50 m s^{-1} and predicted radial velocities less than $\pm 30 \text{ m s}^{-1}$. Thus, both of these models clearly disagree with the observations.

5. DISCUSSION AND CONCLUDING REMARKS

The fundamental reason for the failure of all of the blend scenarios to reproduce the observations for OGLE-TR-56 is that the variations expected in the radial velocities and in the bisector spans from our simulations are *of the same order of magnitude*, and typically differ by a factor of two or less, at least for configurations that are consistent with the light curve constraints. Similar results were reported by Santos et al. (2002). In our case the predicted bisector span variations tend to be larger than the velocity variations. By contrast, the bisector variations actually measured for OGLE-TR-56 are essentially negligible while the velocity variations are highly significant. Thus, no model can reproduce both simultaneously, and our tests show this discrepancy cannot be solved by adjusting the blend parameters. A further reason blend models fail here is the strong observational constraint on the brightness of star 1. A star with only $\sim 3\%$ of the light of star 3 does not produce enough of an effect to be noticeable, either in the line profiles or

in the measured radial velocities. The strong rotational broadening of star 1, as predicted from our light curve fits, only reduces the effect even further. The conclusion must be, then, that a blend configuration involving an eclipsing binary along the same line of sight (whether in a physical triple system, or in the background) cannot account for the observational signatures in OGLE-TR-56 (photometric and spectroscopic), and we are left with a planetary companion in orbit as the only viable explanation. We are unable to devise a more contrived scenario, perhaps involving more stars, that does not go against one or another of the observational constraints.

Dozens of transit candidates are being produced by current deep narrow-field searches that focus on very faint stars, where crowding is potentially a serious issue due to the high stellar densities. Wide-field searches of brighter objects have also entered production mode, and suffer from a similar confusion problem because of the large angular pixel scales. The incidence of blends with a background eclipsing binary in both types of surveys is therefore expected to be rather high. The same is true in most cases for future transit searches from space such as NASA's *Kepler* mission, which will look for even smaller photometric signals produced by Earth-size planets.

The procedures developed in Paper I to model blend light curves in detail, along with those described in §4 to simulate spectral line asymmetries and velocity variations, are powerful analysis tools that can be of great help for validating these transiting planet candidates. The combination of the two techniques makes it possible to construct self-consistent and realistic blend scenarios and to make predictions that can then be tested quantitatively against the observations. The application to OGLE-TR-56 in this paper has provided crucial evidence of its true nature, and serves as an example of follow-up studies that may be applied to other transit candidates.

We are grateful to A. Udalski and the OGLE team for numerous contributions to this project, and to the referee, G. Mallén-Ornelas, for a prompt and careful reading of the manuscript and a number of helpful suggestions. Some of the data discussed herein were obtained at the W. M. Keck Observatory, which is operated as a scientific partnership among the California Institute of Technology, the University of California and the National Aeronautics and Space Administration. The Observatory was made possible by the generous financial support of the W. M. Keck Foundation. G.T. acknowledges support for this work from NASA's *Kepler* mission, STScI program GO-9805.02-A, the Keck PI Data Analysis Fund (JPL 1257943), and NASA Origins grant NNG04LG89G. M.K. gratefully acknowledges the support of NASA through the Michelson fellowship program. S.J. thanks the Miller Institute for Basic Research in Science at UC Berkeley for support through a research fellowship. This research has made use of NASA's Astrophysics Data System Abstract Service.

REFERENCES

Alonso, R., Brown, T. M., Torres, G., Latham, D. W., Sozzetti, A., Mandushev, G., Belmonte, J. A., Charbonneau, D., Deeg, H. J., Dunham, E. W., O'Donovan, F. T., & Stefanik, R. P. 2004, *ApJ*, 613, L153

Baraffe, I., Chabrier, G., Allard, F., & Hauschildt, P. H. 1998, *A&A*, 337, 403

Baraffe, I., Selsis, F., Chabrier, G., Barnam, T. S., Allard, F., Hauschildt, P. H., & Lammer, H. 2004, *A&A*, 419, L13

Bouchy, F., Pont, F., Santos, N. C., Melo, C., Mayor, M., Queloz, D., & Udry, S. 2004, *A&A*, 421, L13

Charbonneau, D., Brown, T. M., Latham, D. W., & Mayor, M. 2000, *ApJ*, 529, L45

Drake, A. J. 2003, *ApJ*, 589, 1020

Drake, A. J., & Cook, K. H. 2004, *ApJ*, 604, 379

Dreizler, S., Hauschildt, P. H., Kley, W., Rauch, T., Schuh, S. L., Werner, K., & Wolff, B. 2003, *A&A*, 402, 791

Etzel, P. B. 1981, in *Photometric and Spectroscopic Binary Systems*, eds. E. B. Carling and Z. Kopal (Dordrecht: Reidel), 111

Gaudi, B. S., Seager, S., & Mallén-Ornelas, G. 2004, *ApJ*, submitted (astro-ph/0409443)

Girardi, L., Bressan, A., Bertelli, G., & Chiosi, C. 2000, *A&AS*, 141, 371

Gray, D. F. 1992, *The Observation and Analysis of Stellar Photospheres*, 2nd Ed. (Cambridge: Cambridge Univ. Press), 417

Gray, D. F. 1997, *Nature*, 385, 795

Gray, D. F. 1998, *Nature*, 391, 153

Gray, D. F., Hatzes, A. P. 1997, *ApJ*, 490, 412

Henry, G. W., Marcy, G. W., Butler, R. P., & Vogt, S. S. 2000, *ApJ*, 529, L41

Horne, K. 2003, in *Scientific Frontiers of research on Extrasolar Planets*, eds. D. Deming and S. Seager (San Francisco: ASP), ASP Conf. Ser., 294, 361

Konacki, M., Torres, G., Jha, S., & Sasselov, D. D. 2003a, *Nature*, 421, 507

Konacki, M., Torres, G., Sasselov, D. D., & Jha, S. 2003b, *ApJ*, 597, 1076

Konacki, M., Torres, G., Jha, S., & Sasselov, D. D., Pietrzyński, G., Udalski, A., Jha, S., Ruiz, M. T., Gieren, W., & Minniti, D. 2004, *ApJ*, 609, L37

Kruszewski, A., & Semeniuk, I. 2003, *Acta Astronomica*, 53, 241

Kurtz, M. J., & Mink, D. J. 1998, *PASP*, 110, 934

Mallén-Ornelas, G., Seager, S., Yee, H. K. C., Minniti, D., Gladders, M. D., Mallén-Fullerton, G. M., & Brown, T. M. 2003, *ApJ*, 582, 1123

Mayor, M., Pepe, F., Queloz, D., Bouchy, F., Rupprecht, G., Lo Curto, G., Avila, G., Benz, W., Berta, J.-L., Bonfils, X., Dall, Th., Dekker, H., Delabre, B., Eckert, W., Fleury, M., Gilliotte, A., Gojak, D., Guzman, J. C., Kohler, D., Lizon, J.-L., Longinotti, A., Lovis, C., Mégevand, D., Pasquini, L., Reyes, J., Sivan, J.-P., Sosnowska, D., Soto, R., Udry, S., Van Kesteren, A., Weber, L., & Weilenmann, U. 2003, *Messenger*, 114, 20

Nelson, B., & Davis, W. 1972, *ApJ*, 174, 617

Pont, F., Bouchy, F., Queloz, D., Santos, N. C., Melo, C., Mayor, M., & Udry, S. 2004, *A&A*, in press (astro-ph/0408499)

Popper, D. M., & Etzel, P. B. 1981, *AJ*, 86, 102

Queloz, D., Henry, G. W., Sivan, J. P., Baliunas, S. L., Beuzit, J. L., Donahue, R. A., Mayor, M., Naef, D., Perrier, C., & Udry, S. 2001, *A&A*, 379, 279

Ribas, I. 2003, *A&A*, 398, 239

Santos, N. C., Mayor, M., Naef, D., Pepe, F., Queloz, D., Udry, S., Burnet, M., Clausen, J. V., Helt, B. E., Olsen, E. H., & Pritchard, J. D. 2002, *A&A*, 392, 215

Sasselov, D. D. 2003, *ApJ*, 596, 1327

Schneider, J. 2004, *The Extrasolar Planet Encyclopaedia*, see web page <http://www.obspm.fr/encycl/encycl.html>

Seager, S., & Mallén-Ornelas, G. 2003, *ApJ*, 585, 1038

Siess, L., Forestini, M., & Dougados, C. 1997, *A&A*, 324, 556

Sirk, E., & Paczyński, B. 2003, *ApJ*, 592, 1217

Torres, G., & Ribas, I. 2002, *ApJ*, 567, 1140

Torres, G., Konacki, M., Sasselov, D. D., & Jha, S. 2004a, *ApJ*, 609, 1071

Torres, G., Konacki, M., Sasselov, D. D., & Jha, S. 2004b, *ApJ*, in press (astro-ph/0406627) (Paper I)

Trilling, D. E., Benz, W., Guillot, T., Lunine, J. I., Hubbard, W. B., & Burrows, A. 1998, *ApJ*, 500, 428

Udalski, A., Paczyński, B., Źebruń, K., Szymański, M., Kubiak, M., Soszyński, I., Szewczyk, O., Wyrzykowski, L., & Pietrzyński, G. 2002a, *Acta Astronomica*, 52, 1

Udalski, A., Źebruń, K., Szymański, M., Kubiak, M., Soszyński, I., Szewczyk, O., Wyrzykowski, L., & Pietrzyński, G. 2002b, *Acta Astronomica*, 52, 115

Udalski, A., Szewczyk, O., Źebruń, K., Pietrzyński, G., Szymański, M., Kubiak, M., Soszyński, I., & Wyrzykowski, L. 2002c, *Acta Astronomica*, 52, 317

Udalski, A., Pietrzyński, G., Szymański, M., Kubiak, M., Źebruń, K., Soszyński, I., Szewczyk, O., & Wyrzykowski, L. 2003, *Acta Astronomica*, 53, 133

Vogt, S. S., Allen, S. L., Bigelow, B. C., Bresee, L., Brown, B., Cantrall, T., Conrad, A., Couture, M., Delaney, C., Epps, H. W., Hilyard, D., Hilyard, D. F., Horn, E., Jern, N., Kanto, D., Keane, M. J., Kibrick, R. I., Lewis, J. W., Osborne, J., Pardeilhan, G. H., Pfister, T., Ricketts, T., Robinson, L. B., Stover, R. J., Tucker, D., Ward, J., & Wei, M. Z. 1994, *Proc. SPIE*, 2198, 362

Yi, S. K., Kim, Y., & Demarque, P. 2003, *ApJS*, 144, 259

Zucker, S., Mazeh, T., Santos, N. C., Udry, S., & Mayor, M. 2003, *A&A*, 404, 775